Ultrasound precipitation of manganese carbonate: the effect of power and frequency on particle properties

Jeroen Jordens, Nico De Coker, Bjorn Gielen, Tom Van Gerven, Leen Braeken

PII: S1350-4177(15)00031-0
DOI: http://dx.doi.org/10.1016/j.ultsonch.2015.01.017
Reference: ULTSON 2787

To appear in: *Ultrasonics Sonochemistry*

Received Date: 19 November 2013
Revised Date: 27 October 2014
Accepted Date: 19 January 2015

Please cite this article as: J. Jordens, N. De Coker, B. Gielen, T. Van Gerven, L. Braeken, Ultrasound precipitation of manganese carbonate: the effect of power and frequency on particle properties, *Ultrasonics Sonochemistry* (2015), doi: http://dx.doi.org/10.1016/j.ultsonch.2015.01.017

Ultrasound precipitation of manganese carbonate: the effect of power and frequency on particle properties

Jeroen Jordens[a,b]*, Nico De Coker[a], Bjorn Gielen[b], Tom Van Gerven[a], Leen Braeken[b]

[a] Department of Chemical Engineering, KU Leuven, De Croylaan 46, B-3001 Leuven, Belgium
[b] Researchgroup Lab4U, Faculty of Industrial Engineering, KU Leuven, Belgium
*Corresponding author. Address: De Croylaan 46, 3001 Leuven; E-mail address: jeroen.jordens@cit.kuleuven.be; tel.: +32 16 32 06 86; fax: +32 16 32 29 91

Abstract

The influence of ultrasonic frequency and intensity on particle shape, tap density and particle size distribution was investigated during the precipitation of manganese carbonate. For the first time, a broad frequency range of 94 till 1135 kHz was studied in one single reactor setup. Smaller and more spherical particles were observed during sonication compared to silent conditions. Lower frequencies and increased intensities result in smaller and more spherical particles. The most spherical particles with superior tap densities are obtained at the lowest frequency and most elevated intensity. Moreover, the results indicate that a particle size threshold exists, below which the particle size cannot be reduced by a further increase of the ultrasonic intensity or reduction of the frequency. Sonication of already formed spherical powders resulted in particles with smaller sizes but unaffected shapes. Finally, one test with pulsed ultrasonic irradiation resulted in equally sized particles with similar sphericity as the ones produced under continuous sonication.

Keywords

ultrasound precipitation, ultrasound shaping, particle engineering, sonochemistry, process intensification

1. Introduction

Precipitation reactions are widely used in industry to manufacture paints, pigments, fine chemicals, pharmaceuticals, polymers, etc. [1-5]. The application of ultrasound during these processes is well studied in literature and has shown effects on both the particle size distribution (PSD) and the particle shape [4, 6-8].

A reduction in PSD of the formed particles by application of ultrasound is observed by several authors [6, 8-11]. This reduction originates from the consecutive formation, growth and collapse of cavitation bubbles and subsequent shock waves, micro jets, increased micro turbulence and elevated local pressures. These effects are well known to both enhance the nucleation rate which results in a larger amount of fine particles, and breakage of the already formed particles into smaller particles by the large shockwaves and micro jets [9, 12-15]. The term grinding will be used in this paper to describe this effect of size reduction.

Besides a size reduction, ultrasound can also induce a shaping effect, namely the formation of spherical particles under sonication [16-19]. Pohl *et al.*, for example, studied the precipitation of $BaSO_4$ in a continuous sonochemical flow reactor [18]. The creation of spherical particles, compared to flat (flaky) particles under silent conditions, was observed by sonication at 20 kHz and 20-160 W. The reactor was a conical reaction chamber with a volume of 10 mL and a residence time between 4.5 - 15 s. The ultrasound precipitation of manganese carbonate from aqueous solutions of NH_4HCO_3 and $MnSO_4$ was investigated by Byrne *et al.* [19]. Also in this case, spherical particles were produced by ultrasonic irradiation at 20 kHz. The power of 400 W, supplied to the ultrasonic horn, was, however, significantly higher than the 20-160 W in the paper of Pohl *et al*.

Although the exact mechanism behind ultrasound shaping is still unknown, there are two commonly used theories reported in literature. The first one assigns the increased sphericity of the particles to the improvement in mass transfer rate between solution and surface [20]. Ultrasonic irradiation creates cavitation bubbles which collapse, resulting in microscopic turbulence and thinning of the hydrodynamic boundary layer around the particles. It is believed that these effects are responsible for an enhanced mass transfer in the mixture, therefore increasing the possibility of the solute molecules to combine with each other and approach each side of the growing particle more uniformly and easily [21]. The second theory explains the formation of spherical particles by the melting of particles upon implosion of the cavitation bubbles [10, 22-24]. Collapsing cavitation bubbles create intense shock waves which cause high velocity collisions of solid particles. These collisions result in extreme heating at the point of impact and as a result the particles are melted together [24]. The creation of agglomerates with smooth surfaces was observed during the sonication of Sn, Zn, Cu, Ni, Fe, and Cr slurries [7, 24].

While several studies are performed on ultrasound assisted precipitation, the impact of the frequency and intensity is rarely investigated and no conclusions can be drawn. Zhang *et al.* tested the effect of ultrasound at 20 and 33 kHz during the precipitation of $Al(OH)_3$ [6]. At both frequencies, an acceleration of secondary nucleation was observed with the largest effect at 33 kHz. The mean size of the particles was also smaller at the frequency of 33 kHz compared to the ones at 22 kHz. The weight percentage of fine particles with sizes less than 20 µm increased from 8.3 to 25.9 % and 30.3% after 12h of sonication at 20 and 33 kHz, respectively. In the same period, ultrasound had decreased the amount of 40-60 µm crystals with 10% and enlarged the amount of crystals larger than 100 µm by 8-10%. This effect was attributed to the collision and agglomeration of coarse particles by ultrasound. These results indicate that the frequency of 33 kHz is preferable compared to 20 kHz. It should, however, be noted that the power transferred from the ultrasound source to the liquid was not measured

during these experiments. Therefore the possibility exists that the power transferred from the ultrasonic source to the liquid was not the same for both frequencies. In the same paper, the effect of the ultrasonic power on the precipitation ratio, the percentage of decomposition of the supersaturated sodium aluminate solution, was investigated. An increase of this precipitation ratio was observed with augmentation of the ultrasonic power up to 286 W, but with a further increase of the power to 308 W a decrease was found. This was explained by the decoupling of the sonotrode caused by the coalescence of cavitation bubbles which will form a gas layer between the liquid and the ultrasonic source. As a result, a phase lag between the motion of the liquid and that of the ultrasound source is induced and the ultrasonic source is not able to remain in contact with the liquid during the whole acoustic cycle. Consequently, there is a loss of power transferred from the source to the liquid [6, 25, 26].
Kaully *et al.* patented a method for the creation of spherical particles with smooth and rounded surfaces by ultrasonic treatment of a slurry [9]. The precipitation of cyclotrimehylenetrinitramine (RDX) was studied at frequencies of 25 and 40 kHz and intensities of 10 to 50 W/L. Both shaping (the creation of more spherical particles) and grinding (a reduction in particle size) were observed in varying ratios during these experiments. It was reported that shaping preferred frequencies above 40 kHz, while grinding was dominant at frequencies below 25 kHz. An explanation of these observations was, however, not provided and similar observations are, to the best of our knowledge, not reported elsewhere. In contrast, Li *et al.* observed no impact of sonication at 15, 20, 25 or 30 kHz on the shape, mean size and the size distribution during the salting out of spectinomycin hydrochloride particles [21]. The studied frequency range of 15 till 30 kHz was however considerably smaller and the applied ultrasonic intensities of 26666 W/L significantly higher compared to the patent of Kaully *et al*. It was thought that the wavelengths are much larger at these frequencies than the size of the nuclei and consequently the effects of the sonication are similar at all frequencies. This is, however, also the case in the patent of Kaully *et al.* as in both cases water was used as the solvent, similar frequencies are used and the largest particles were about 150 µm. More recently, Lee *et al.* investigated the effect of ultrasonic frequencies of 20, 44, 139, 500 and 647 kHz on the antisolvent crystallization of sodium chloride [27]. Similar size distributions were observed among the different frequencies. Slightly larger and more cubic crystals were, however, visible during sonication at 500 and 647 kHz compared to the lower frequencies. The enlarged abrasion and attrition by intense shear effects at low ultrasonic frequencies were thought to cause this change in crystal shape.

The above mentioned papers made different observations about the effect of the frequency and intensity on particle properties such as the size or shape. Furthermore, different reactor geometries, products, ultrasonic powers and frequencies are used. Therefore, it's not possible to draw a general conclusion. The purpose of this paper is to investigate the impact of the ultrasonic frequency and intensity on the shaping and grinding during the precipitation of manganese carbonate. In contrast to previous articles, the frequency will be investigated over a broad range of 94 till 1135 kHz in one single reactor geometry and one single product. The power transferred from the ultrasonic source to the liquid will also be calibrated. Furthermore, the effect of the ultrasonic intensity on the particle size, shape and tap density will be investigated at the minimum and maximum frequency of 94 and 1135 kHz. Some additional tests will be performed to investigate the effect of the insonation time and test the possibility of shaping already formed particles.

2. Materials and methods

2.1. Experimental setup

All experiments were carried out in a glass unbaffled continuous stirred tank reactor (CSTR). Figure 1 shows the reactor setup, which consists of a glass jacketed cylinder flanged between an ultrasound transducer at the bottom and a glass cover at the top. This cover contains 4 holes for the mixer, temperature probe and two reactor inlets. The reactor had an inner diameter of 55 mm and the outlet of the reactor was positioned at 80 mm above the bottom. The temperature was controlled by a Julabo MP thermostatic bath and a VWR EU 620-0917 digital thermometer, with an accuracy of ±1°C, was inserted to check the operating temperature. The solution was mixed during all experiments by a Cole-Parmer EW-50006-01 agitator at a constant stirring speed of 800 rpm. The latter was equipped with a 30 mm diameter stainless steel axial blade impeller, mounted 10 mm above the reactor bottom.
Two different ultrasound transducers were used, one with a resonance frequency of 94 kHz (Ultrasonics World MPI-7850D-20_40_60H), another with frequencies of 577 and 1135 kHz (Meinhardt E/805/T/M). The first transducer was glued to a glass plate to avoid corrosion and erosion of the transducer surface. The latter one was a titanium transducer which could directly be used. Both transducers are chosen for their similar dimensions which differ only 3 mm. The Ultrasonics World transducer has a diameter of 78 mm compared to 75 mm for the Meinhardt transducer.
The ultrasonic frequency and power were controlled by a Picotest G5100A waveform generator connected to an E&I 1020L RF power amplifier which drives the ultrasound transducers.
Two pulse-free LaboCat HPLH 200 PF pumps were used to inject the reactants into the reactor vessel. Both inlets were positioned 15 mm above the outlet of the reactor such that the reactants were added by surface addition. The actual flow rates of the pumps were 7.77 mL/min and 8.05 mL/min for respectively the $MnSO_4$ and Na_2CO_3 solutions. The average residence time was about 12 min and the reaction volume 190 mL.

2.2. Chemicals

Manganese sulfate monohydrate with a purity of at least 97 % (Chem Lab NV) and sodium carbonate anhydrate with a purity above 99.5 % (Hawkins Inc.) were used to create aqueous solutions of 1.74 mol/L and 1.76 mol/L, respectively. These concentrations were chosen to obtain a molar ratio of 1.05 for Na_2CO_3 : $MnSO_4$, taking into account the actual flow rates of both pumps. Ultra pure water (18 MOhm.cm) was used to make the solutions. The manganese sulfate solutions were filtered over a 2.5 µm filter to remove impurities.

2.3. Calorimetric power measurements

Different ultrasonic transducers can have variations in the ultrasonic field or the efficiency of power transfer. To minimize these differences, the power transferred from the transducer into the liquid was calibrated by calorimetry. Controlling the calorimetric power allows to correlate the results among different frequencies. The importance of these calorimetric measurements is already emphasized in literature [7, 28, 29]. It should, however, be noted that other variations among the different transducers, like differences in the ultrasonic field, are still possible.

First, the resonance frequencies of the transducers were defined by a Sine Phase impedance analyzer 16777K. Prior to these measurements, the transducers were clamped to the reactor, the reactor was filled with ultra pure water and the liquid was stirred at 800 rpm and heated to 60°C. Second, the power dissipated to the liquid was calibrated for all transducers by calorimetry. Before the start of the measurements, the reactor was insulated by a fiberglass blanket to minimize heat losses to the environment and the water was heated to 60°C. Upon reaching a stable temperature, the thermostatic bath was turned off and ultrasound was switched on. To correct for heat losses to the environment, the temperature decrease under silent conditions (6.6°C after 10 min) was also measured and taken into account during calculations. The calorimetric power was calculated over 10 min using Eq. 1 and the temperature increase relative to the temperature under silent conditions was used for all calculations.

Eq. 1 $$P_{cal} = \frac{dT}{dt} c_p m$$ [30]

with P_{cal} the calorimetric power (W), T the temperature (K), t the time (s), c_p the heat capacity of water (J/(g K)) and m the mass of water (g). The value of c_p was set at 4.18 J/(g K) and m was 137 and 175 g for respectively the 94 kHz and 577-1135 kHz transducer.

In all cases, a linear relationship between the power transferred to the transducer and the calorimetric power was observed with a linear correlation coefficient (r^2) of at least 0.96.

2.4. Experimental procedure precipitation reaction

Before the start of the experiment, 20 mL ultra pure water was added to the reactor to allow proper temperature control and mixing of the reactants from the start. The experiment was started by turning on the pumps and the ultrasonic irradiation. The reaction temperature was kept constant at 60°C ±0.2°C after reaching steady state and the stirring speed was set at 800 rpm for all experiments. Lipowska showed that mixing can be assumed ideal in a continuous stirred tank reactor when V*/Q<0.2 [31]. Where V* is the volumetric flow rate of the inlets (15.82 mL/min) and Q the impeller pumping capacity (cm³/min) given by $Q = 2.3\ n\ d_m^2 b$. Here, n is the impeller speed (800 rpm), d_m the impeller diameter (30 mm) and b the impeller height (8 mm) resulting in a Q of 13248 cm³/min. Consequently, V*/Q becomes 0.0012 which is considerably lower than 0.2 so it can be assumed that the reactor is perfectly mixed.

Samples of 5 mL were taken at the reactor outlet after 5, 20, 40, 60, 80, 100 and 120 min. No blockage or accumulation of the reactor outlet was observed. These samples were quenched in 100 mL ultra pure water to stop the precipitation reaction and avoid agglomeration or Ostwald ripening of the particles. The particle size distribution (PSD) of these samples was measured by a Malvern Mastersizer S with MS14 sample dispersion unit.

Additional samples of 10 mL were taken after 60 and 120 min, filtered over a 0.45 µm Millipore filter, washed with ultrapure water and dried in an oven at 40°C for 24 hours. These samples were used to analyze the particle morphology and also, the particle size of these filtrated samples was compared to the ones obtained by quenching to ensure that no errors were made during quenching. No significant differences in particle size were detected during all experiments, thereby confirming the reliability of the quenching method. The morphology of the $MnCO_3$ particles was analyzed with a Philips XL30 FEG scanning electron microscope (SEM). Finally, the experiment was stopped after 120 min and the reactor content was filtered

over a general purpose laboratory filter (MN 713 1/4), washed with ultra pure water and dried at 40°C for 24 hours. This sample was used for analysis of the mineralogy and tap density. Mineralogical analysis was conducted by a Philips PW1830 X-ray diffractometer and DiffracPlus software. The tap density, a measure for the density of a packed powder, is an often used powder characteristic in pharmaceutical, food, packaging and metallurgic industry [32, 33]. This tap density was analyzed by filling a 25 mL graduated cylinder with a known mass of powder, tapping 4000 times with a tap density tester (Erweka SVM201) and reading the volume of the tapped powder from the graduated cylinder.
Furthermore, a test was performed to investigate the effect of the insonation time on the particle size, shape and tap density. Ultrasonic irradiation was applied at a frequency of 577 kHz and similar power settings as during the continuous experiment. The duty cycle was reduced to 50%; with a pulse time of 86.7 ms on a total period of 173.3 ms. The same procedure as in the continuous experiments was followed.
The sonicated experiments were repeated twice at each frequency and power to ensure reproducible results. The final samples of the duplicate tests were combined and mixed together to achieve sufficient sample for the measurements of the tap densities. Silent experiments were performed as a reference case and repeated three times.

2.5. Procedure for testing effect ultrasound on existing particles

One test was performed to check the effect of ultrasound sonication on already formed $MnCO_3$ particles. The reactor was first filled with a 100 g/L $MnCO_3$ powder solution with a median diameter of 49 µm. These $MnCO_3$ particles were prepared under silent conditions as described in 2.4. The solution was then heated to 60°C and stirred at 800 rpm to ensure the same operating conditions as in the precipitation experiments. Next, the experiment was started by switching on ultrasound at a frequency of 94 kHz and an intensity of 49 W/L. Samples of 5 mL were taken every minute for a total time of 15 min and quenched in 100 mL deionized water. The irradiation time was set at 15 min to ensure a similar residence time in the reactor as compared to the previous precipitation tests. Afterwards, these samples were filtered over a 0.45 µm Millipore filter, washed with deionized water and dried in an oven at 40°C for 24 h. SEM images were taken from these samples to analyze the morphology of the particles. Finally, the experiment was stopped after 15 min and a sample of 10 mL was taken and quenched in 100 mL deionized water for PSD analysis. To compensate for the volume reduction by sampling, the ultrasonic power was reduced every minute to keep the ultrasound intensity constant at 49 W/L.

3. Results and discussion

3.1. Influence of the frequency

Figure 2 shows the median particle diameter as function of the reaction time for the applied frequencies. Ultrasound didn't affect the time to reach steady state since the median particle diameter stabilizes after 60 min at both sonicated and silent conditions. This diameter was, however, significantly reduced from 48 µm to 13-19 µm by applying ultrasound. No significant differences in the median diameter were observed among the sonicated experiments at 49 W/L. The PSD of the final samples is given in Figure 3. A bimodal distribution appears for all experiments. The first peak of fine particles is visible around 0.3 µm and remains constant in size. The amount of fines produced increases by application of ultrasound but remains constant at the different frequencies. The increase in the amount of fines by applying ultrasound is likely to be attributed to fragmentation of already formed particles [6, 34-36]. The second peak in Figure 3 consists of larger particles and accounts for the majority of the particles in the reactor. The size of these particles shifts from 60 to about 19 µm, regardless of the applied frequency. The reduction in median particle size by sonication observed in Figure 2 is therefore primarily caused by the reduced particle size of these larger particles. As a result, one can conclude that smaller particles are created by sonication, whose size is independent of the applied frequency at an ultrasonic intensity of 49 W/L. Similar observations were also reported in literature. Liu *et al.* investigated the precipitation of sodium aluminate during sonication and observed a strong reduction in particle size at 16 kHz, while sonication at 33 and 50 kHz had little effect on the particle size distribution [34]. No calorimetric power calibration was, however, performed which makes it difficult to draw conclusions from these observations. Such a power calibration was performed by Lee *et al.* during the study of the effect of the ultrasonic frequency on the antisolvent crystallization of sodium chloride [27]. The authors observed that the particle size was reduced to the same extent by ultrasound between 20 and 645 kHz. They suggested that at the studied power level, the threshold for the particle size has already been reached and therefore no further changes were observed when varying the frequency. This hypothesis will be further discussed in section 3.2 where different power levels are tested.

Figure 4 shows the SEM images of the samples produced under silent and ultrasonic conditions at 94, 577 and 1135 kHz. The particles prepared under sonication are significantly more spherical compared to the silent ones. The lower the applied frequency, the more spherical the particles become.

Figure 5 shows the improvement in tap densities compared to silent conditions (1.09 g/cm³). Applying ultrasound resulted in all cases in a significant increase of this value. The maximum enhancement of 91% is achieved at a frequency of 94 kHz, higher frequencies resulted in smaller improvements. Therefore, one could state that lower frequencies are preferred whenever superior powder densities are required. The obtained tap densities of 1.88 - 2.08 g/cm³ are comparable to the 1.7 - 2.3 g/cm³ reported by Byrne *et al.* [19]. These values are also obtained during the precipitation of $MnCO_3$, but the applied frequency of 20 kHz was lower than the 94 kHz used in this paper. Also, an ultrasonic horn was used instead of a transducer placed at the bottom. The most significant difference is, however, the ultrasonic intensity. A range of 800 to 8000 W/L was applied in the paper of Byrne *et al.* compared to 49 W/L during the experiments shown in Figure 5. It should be noted that in the paper of Byrne *et al.* the power supplied to the ultrasonic horn is reported and not the real power inside the reactor. The efficiency for energy transfer between the ultrasound source and the liquid is typically about 30 % [15, 28]. Taking this into account, one could estimate that the real power intensity inside the reactor will be about 240-2400 W/L. This is still one order of magnitude

higher than the 49 W/L used here. The lack of mechanical stirring in the research of Burne *et al.* is hypothesized to cause this difference. In literature, it is believed that strong mixing is favorable during the precipitation process because it allows uniform supersaturation levels. As a result, homogeneous isotropic crystal growth of the nuclei occurs and spherical shaped particles with uniform size distributions will be produced [37]. Mechanical agitation provides mainly macroscopic mixing. In this way, the formed particles are distributed homogeneously and sedimentation of the slurry is avoided. On a molecular level, however, the molecules are not distributed rapidly and uniformly over the solution. Therefore, this type of mixing does not allow to produce a uniform level of supersaturation in a short time scale. As a result, the formed particles are more rough and less rounded which will result in lower tap densities. Ultrasound, in contrast, creates shockwaves by the implosion of cavitation bubbles and consequently microscopic turbulence and micro-streaming [38, 39]. This micro-mixing allows increased mass transfer among the reactants and products, thus enhancing the nucleation and growth rates [21]. When macro-mixing is, however, not sufficient and the particles are not distributed uniformly over the reactor, it can be expected that the beneficial effects of ultrasound are reduced. Therefore, one could state that both macro- and micro mixing are required for an efficient precipitation process, where the former is most efficiently produced by mechanical agitation and the latter by ultrasonic irradiation. It should be noted that too much mechanical agitation can also disturb the pressure fields by scattering of the ultrasound waves [40]. To exclude these effects, some calorimetric tests were performed at different stirring speeds. Figure 6 shows the calorimetric power as function of the stirring speed. No significant variation is visible between the stirring speeds of 50 and 1000 rpm. These results indicate that the amount of power transferred from the ultrasonic source to the liquid remains constant at these speeds. Therefore it can be assumed that the amount of scattering at a speed of 800 rpm is rather limited.

Furthermore, XRD analyses showed the formation of rhodochrosite $MnCO_3$ particles with lattice constants a= 4.777 Å and c = 15.670 Å. These values are consistent with values reported in literature [5].

As a conclusion, lower ultrasonic frequencies result in more spherical particles, improved tap densities and slightly smaller median particle diameters. The impact of the frequency on the particle size seems to be rather limited at an intensity of 49 W/L as the size and amount of both fines and larger particles is similar. Comparison of the results obtained here and the ones reported in literature indicate that both mechanical and ultrasound mixing are preferable for an energy efficient production of particles with superior tap densities.

3.2. Influence of the intensity

The effect of the ultrasonic intensity on the produced particles was tested for the frequencies of 94 and 1135 kHz. Steady state was again reached after 60 min, regardless of the ultrasonic intensity. Figure 7 show the PSD of 94 and 1135 kHz at ultrasonic intensities of 4-5, 25 and 49 W/L. The formation of smaller particles is, for both frequencies, visible at more elevated intensities. The volume percentage of the first peak increases with augmentation of the ultrasonic intensity up to 2.8% and 2.0% at respectively 94 kHz and 1135 kHz. The particle size of these fine particles remains, nevertheless, constant at 0.3 µm. The particle size of the second peak, in contrast, reduces significantly with increasing ultrasonic intensities. The maximum particle size of 52 µm, obtained under silent conditions, was for example reduced to 17 µm under ultrasonic irradiation of 1135 kHz at 49 W/L. This reduction in particle size

with increasing ultrasonic intensities is also reported by several other authors [6-10, 15, 38, 41]. A strong increase in the nucleation rate, breakage of agglomerates by shockwaves and micro jets, and strong enhancement of the convection in the vicinity of the particle surface are thought to cause this reduction in size. This augmentation of the convection reduces the thickness of the diffusional layer, thereby increasing the mass transfer rate. As a result, smaller and more uniform particles are produced under ultrasound irradiation compared to mechanical agitation [41]. From Figure 7, one can see that the second peak reaches a minimum around 17 µm. This minimum is reached at 25 W/L and 94 kHz. A further increase of the ultrasonic intensity to 49 W/L did not lead to a further decrease of this size. This observation is in agreement with the hypothesis made by Lee et al. that a particle size threshold exists below which particles cannot be reduced [27].
When comparing the different frequencies in Figure 7, one can see that the PSD of 94 and 1135 kHz is comparable at 49 W/L; while at 4-25 W/L, the PSD of 94 kHz is considerable smaller than the one of 1135 kHz. The observations made at 4-25 W/L can be explained by the effect of the frequency on the nucleation rate, shockwaves, micro jets and convection. Low ultrasonic frequencies will result in higher nucleation rates and hence are likely to produce more but smaller particles [34, 42]. Also, the implosions of the cavitation bubbles are more violent at low frequencies which result in more intense shockwaves, micro jets and stronger enhancement of convection [15, 43]. At 49 W/L, however, the threshold value of 17 µm was already reached at 1135 kHz so no significant reduction in size could be achieved by reducing the frequency to 94 kHz. This is, again, in agreement with the hypothesis of Lee *et al.* that a particle size threshold value exists.

The same minimum particle size threshold seems to exist for the first peak of fine particles. In all our experiments, the peak of fine particles remains constant at around 0.3 µm and no particles smaller than 0.1 µm are observed. Similar observations were also made during other sonication experiments with solid particles performed in our research group. It is hypothesized that a minimum particle size exists at which size reduction will not occur anymore. As described before, the observed grinding effects are likely caused by breakage of the large particles in smaller ones by shockwaves, microjets or high velocity interparticle collisions [15]. The first possibility is that particles break into smaller parts by the stresses induced on the crystal lattice by the shockwaves. This breakage occurs typically when defects are present in the crystal lattice. The chance of breakage of small particles is, however, considerably smaller compared to large particles as a significantly minor amount of defects are present in the crystal lattice. Therefore it's already believed in literature that breakage of small particles due to ultrasonic induced shockwaves is very unlikely [44]. The second option is that of breakage due to microjets. This occurs when cavitation bubbles collapse asymmetrically because of the presence of a solid surface. This will result in the creation of high speed microjets towards the particle surface [15, 24]. In literature, it is, however, believed that the formation of microjets is avoided as long as the diameter of the particles is smaller than the diameter of the cavitation bubbles [24]. At the maximum frequency of 1135 kHz, the diameter of the cavitation bubbles will be around 2.6 µm [43, 45]. Therefore, it can be assumed that the formation of microjets and consecutive breakage of the particles will not occur for fine particles with diameters around 0.3 µm. Finally, sonication of a powder mixture in water can accelerate the particles to velocities about 80 m/s [24]. When these particles collide with these high velocities, they can induce breakage of the particles. Particles with diameters below 20 µm are, however, thought not to be accelerated by cavity expansion because the momentum achieved by the pressure drop across their surface is relatively small [46]. Moreover, small particles have a significant smaller relaxation time compared to larger particles. Hence, it was concluded by Wagterveld *et al.* that the large aggregates are likely to

be broken in smaller parts but that breakage of small single crystals is not common [44]. These conclusions reported in literature support our hypothesis that particle breakage by sonication occurs up to a certain limit. When the particles are too small, size reduction will not occur anymore.

The SEM images of particles produced at both 94 and 1135 kHz, show an increased sphericity of the particles at elevated ultrasonic intensities. As an example, the SEM images at the frequency of 94 kHz are given in Figure 8. From this figure, one can see that at an intensity of 4 W/L, the particles still resemble the aggregates formed under silent conditions but the surface is somewhat smoother. The $MnCO_3$ particles formed at 25 and 49 W/L both approach sphericity with the smoothest surfaces obtained at the latter intensity. The tap densities reported in Figure 5 confirm this trend as the maximum values are observed at the highest intensities for both frequencies. The difference in tap density between the intensities of 25 and 49 W/L is less pronounced as the ones between 4 and 25 W/L. Although the particle size threshold is reached, the particle shape and tap density can still be affected by increasing the intensity as can be seen in Figures 5 and 8.

3.3. Influence of the insonation time

One test was performed with pulsed ultrasonic irradiation at a frequency of 577 kHz and similar power settings as during the continuous experiment. The observed time to steady state and PSD are comparable to the ones obtained under continuous irradiation. Also, the SEM images, given in Figure 9, show no significance difference in sphericity of the particles. These results suggest that pulsed ultrasound has potential to improve the efficiency of the process further. More experiments are, however, needed to define the optimal pulse parameters like pulse on- and off time.

3.4. Effect of sonication of already formed particles

Finally, one experiment was performed in batch mode to investigate the effect of sonication on already formed particles. Figure 10 shows the PSD of the samples taken before and after 15 min sonication. Similar to the previous experiments, the peak of fines enlarges while the second peak shifts towards smaller particle diameters. The SEM images provided in Figure 11 show that the particle shape remains unchanged. All SEM images show loosely aggregated particles as obtained in the silent experiments. As a conclusion, one could state that sonication of already formed spherical particles result in smaller particles but has no effect on the shape of these particles. Within the studied reactor setup and process conditions, reactants should be present and thus simultaneous synthesis and formation of the particles should occur to allow shaping of the particles. Shaping without the presence of these reactants does not occur within the studied conditions. It should be noted that the reactor volume was not constant during these tests because of the samples taken for analysis. At the end of the experiment, the liquid height was lowered with 15mm compared to the start. The ultrasonic intensity was kept constant by adapting the power to the volume but because of the change in this liquid height, it cannot be excluded that the ultrasonic field changed.

4. Conclusion

The effect of the ultrasonic frequency and intensity on the particle size and shape of $MnCO_3$ particles was investigated over a frequency range of 94 till 1135 kHz. Low ultrasonic frequencies and high intensities are preferred for the production of spherical particles with superior tap densities. The results obtained in this research indicate that a minimum particle size exists, for both fine and large particles. When working above this particle size threshold, lower frequencies and higher intensities result in smaller particles. When this threshold is reached, the particle size remains unaffected regardless of the used frequency or intensity. The particle shape can, however, still be affected by the ultrasonic intensity or frequency. This threshold can explain why some authors in literature report differences in particle size among different frequencies where others do not. It is important to pay attention to this threshold in future experiments when comparing the effect of ultrasonic frequencies or intensities on the particle size.

Also, it was put forward that both mechanical and ultrasound mixing are required for an energy efficient production of spherical particles with superior tap densities. In addition, the effect of the insonation time was investigated. Pulsed ultrasonic irradiation resulted in particles with similar sphericity and sizes compared to the ones produced by the continuous mode. This create opportunities to improve the efficiency of the process further. Experiments on the sonication of already formed spherical particles indicate that ultrasound should be applied during the precipitation process to affect the particle shape.

Acknowledgements:

The research leading to these results has received funding from the European Community's Seventh Framework Programme (*FP7/2007-2013*) under grant agreement n° NMP2-SL-2012-309874 (ALTEREGO). Research was funded by a Ph.D. grant of the Agency for Innovation by Science and Technology in Flanders (IWT).

References

[1] J.W. Mullin, Crystallization and Precipitation, in: Ullmann's Encyclopedia of Industrial Chemistry, Wiley-VCH Verlag GmbH & Co. KGaA, 2000.
[2] A.S. Myerson, Handbook of Industrial Crystallization, 1993.
[3] N. Jongen, M. Donnet, P. Bowen, J. Lemaître, H. Hofmann, R. Schenk, C. Hofmann, M. Aoun-Habbache, S. Guillemet-Fritsch, J. Sarrias, A. Rousset, M. Viviani, M.T. Buscaglia, V. Buscaglia, P. Nanni, A. Testino, J.R. Herguijuela, Development of a Continuous Segmented Flow Tubular Reactor and the "Scale-out" Concept – In Search of Perfect Powders, Chemical Engineering & Technology, 26 (2003) 303-305.
[4] P. Jeevanandam, Y. Koltypin, A. Gedanken, Synthesis of Nanosized α-Nickel Hydroxide by a Sonochemical Method, Nano Letters, 1 (2001) 263-266.
[5] X. Duan, J. Lian, J. Ma, T. Kim, W. Zheng, Shape-Controlled Synthesis of Metal Carbonate Nanostructure via Ionic Liquid-Assisted Hydrothermal Route: The Case of Manganese Carbonate, Crystal Growth & Design, 10 (2010) 4449-4455.
[6] B. Zhang, J. Li, Q. Chen, G. Chen, Precipitation of Al(OH)3 crystals from supersaturated sodium aluminate solution irradiated with ultrasonic sound, Minerals Engineering, 22 (2009) 853-858.
[7] L.H. Thompson, L.K. Doraiswamy, Sonochemistry: Science and Engineering, Industrial & Engineering Chemistry Research, 38 (1999) 1215-1249.
[8] M.A. Alavi, A. Morsali, Syntheses and characterization of Mg(OH)2 and MgO nanostructures by ultrasonic method, Ultrasonics Sonochemistry, 17 (2010) 441-446.
[9] T. Kaully, B. Keren, T. Kimmel, O. Dekel, Method and apparatus for shaping particles by ultrasonic cavitation, in: R.-A.D.A. LTD. (Ed.) United Stated Patent Application Publication, Israel (IL), 2001.
[10] L.-X. Yang, Y.-J. Zhu, H. Tong, W.-W. Wang, Submicrocubes and highly oriented assemblies of MnCO3 synthesized by ultrasound agitation method and their thermal transformation to nanoporous Mn2O3, Ultrasonics Sonochemistry, 14 (2007) 259-265.
[11] S. Cabanas-Polo, K.S. Suslick, A.J. Sanchez-Herencia, Effect of reaction conditions on size and morphology of ultrasonically prepared Ni(OH)2 powders, Ultrasonics Sonochemistry, 18 (2011) 901-906.
[12] G. Ruecroft, D. Hipkiss, T. Ly, N. Maxted, P.W. Cains, Sonocrystallization: The Use of Ultrasound for Improved Industrial crystallization, Organic Process Research & Development, (2005) 923-932.
[13] R.S. Dhumal, S.V. Biradar, A.R. Paradkar, P. York, Particle engineering using sonocrystallization: Salbutamol sulphate for pulmonary delivery, International Journal of Pharmaceutics, (2009) 129–137.
[14] A. Abbas, M. Srour, P. Tang, H. Chiou, H.-K. Chan, J.A. Romagnoli, Sonocrystallisation of sodium chloride particles for inhalation, Chemical Engineering Science, 62 (2007) 2445-2453.
[15] C. Horst, P.R. Gogate, A.B. Pandit, Ultrasound Reactors, in: Modeling of Process Intensification, Wiley-VCH Verlag GmbH & Co. KGaA, 2007, pp. 193-277.
[16] Ovshinsky, Ultrasonic method for forming spherical nickel hydroxide, in: E.c.d. inc. (Ed.) World intellectual property organization, US, 1996.
[17] Ovshinsky, Active nickel hydroxide material having controlled water content, in: e.c.d. inc. (Ed.) World intellectual property organization, US, 1997.

[18] B. Pohl, R. Jamshidi, G. Brenner, U.A. Peuker, Experimental study of continuous ultrasonic reactors for mixing and precipitation of nanoparticles, Chemical Engineering Science, 69 (2012) 365-372.
[19] T. Byrne, M.P. Dahal, Transition metal compound particles and methods of production, in, WO Patent 2,012,088,604, 2012.
[20] H. Li, H. Li, Z. Guo, Y. Liu, The application of power ultrasound to reaction crystallization, Ultrasonics Sonochemistry, 13 (2006) 359-363.
[21] H. Li, J. Wang, Y. Bao, Z. Guo, M. Zhang, Rapid sonocrystallization in the salting-out process, Journal of Crystal Growth, 247 (2003) 192-198.
[22] T. Prozorov, R. Prozorov, K.S. Suslick, High Velocity Interparticle Collisions Driven by Ultrasound, Journal of the American Chemical Society, 126 (2004) 13890-13891.
[23] K.S. Suslick, S.J. Doktycz, E.B. Flint, On the origin of sonoluminescence and sonochemistry, Ultrasonics, 28 (1990) 280-290.
[24] S.J. Doktycz, K.S. Suslick, Interparticle collisions driven by ultrasound, Science, 247 (1990) 1067-1069.
[25] N.P. Vichare, P. Senthilkumar, V.S. Moholkar, P.R. Gogate, A.B. Pandit, Energy Analysis in Acoustic Cavitation, Industrial & Engineering Chemistry Research, 39 (2000) 1480-1486.
[26] G.J. Price, M.F. Mahon, J. Shannon, C. Cooper, Composition of Calcium Carbonate Polymorphs Precipitated Using Ultrasound, Crystal Growth & Design, 11 (2010) 39-44.
[27] J. Lee, M. Ashokkumar, S.E. Kentish, Influence of mixing and ultrasound frequency on antisolvent crystallisation of sodium chloride, Ultrasonics Sonochemistry, 21 (2014) 60-68.
[28] A. Kordylla, S. Koch, F. Tumakaka, G. Schembecker, Towards an optimized crystallization with ultrasound: Effect of solvent properties and ultrasonic process parameters, Journal of Crystal Growth, 310 (2008) 4177-4184.
[29] Q.P. Isariebel, Sonolysis of levodopa and paracetamol in aqueous solutions, Ultrasonics Sonochemistry, 16 (2009) 610.
[30] J. Raso, P. Mañas, R. Pagán, F.J. Sala, Influence of different factors on the output power transferred into medium by ultrasound, Ultrasonics Sonochemistry, 5 (1999) 157-162.
[31] L. Lipowska, The influence of geometric parameters on the ideal mixing range of liquid in a continuous flow stirred tank reactor, Chemical Engineering Science, 29 (1974) 1901-1908.
[32] Z. Chen, J.R. Dahn, Reducing Carbon in LiFePO4□/□ □C□ Composite Electrodes to Maximize Specific Energy, Volumetric Energy, and Tap Density, Journal of The Electrochemical Society, 149 (2002) A1184-A1189.
[33] V.I. Corporation, Tap Density Test Apparatus, in, IndiaMART InterMESH Limited 2013.
[34] J.-b. LIU, J.-q. CHEN, Z.-l. YIN, P.-m. ZHANG, Q.-y. CHEN, Effect of Ultrasound Frequency on the Precipitation Process of Supersaturated Sodium Aluminate Solution [J], The Chinese Journal of Process Engineering, 2 (2004).
[35] M.D. Luque de Castro, F. Priego-Capote, Ultrasound-assisted crystallization (sonocrystallization), Ultrasonics Sonochemistry, 14 (2007) 717-724.
[36] R. Chow, R. Blindt, R. Chivers, M. Povey, A study on the primary and secondary nucleation of ice by power ultrasound, Ultrasonics, 43 (2005) 227-230.
[37] H. Zhu, E.W. Stein, Z. Lu, Y.M. Lvov, M.J. McShane, Synthesis of Size-Controlled Monodisperse Manganese Carbonate Microparticles as Templates for Uniform Polyelectrolyte Microcapsule Formation, Chemistry of Materials, 17 (2005) 2323-2328.
[38] L.C. Hagenson, L.K. Doraiswamy, Comparison of the effects of ultrasound and mechanical agitation on a reacting solid-liquid system, Chemical Engineering Science, 53 (1998) 131-148.

[39] F. Parvizian, M. Rahimi, N. Azimi, Macro- and micromixing studies on a high frequency continuous tubular sonoreactor, Chemical Engineering and Processing: Process Intensification, 57–58 (2012) 8-15.
[40] V.S. Sutkar, P.R. Gogate, Design aspects of sonochemical reactors: Techniques for understanding cavitational activity distribution and effect of operating parameters, Chemical Engineering Journal, 155 (2009) 26-36.
[41] Y.H. Kim, K. Lee, K.K. Koo, Y.G. Shul, S. Haam, Comparison Study of Mixing Effect on Batch Cooling Crystallization of 3-Nitro-1,2,4-triazol-5-one (NTO) Using Mechanical Stirrer and Ultrasound Irradiation, Crystal Research and Technology, 37 (2002) 928-944.
[42] J. Jordens, B. Gielen, L. Braeken, T. Van Gerven, Determination of the effect of the ultrasonic frequency on the cooling crystallization of paracetamol, Chemical Engineering and Processing: Process Intensification.
[43] L.A. Crum, T.J. Mason, J.L. Reisse, K.S.S. (Eds.), Sonochemistry and sonoluminescence, Kluwer Academic Publishers, Dordrecht, 1997.
[44] R.M. Wagterveld, H. Miedema, G.-J. Witkamp, Effect of Ultrasonic Treatment on Early Growth during CaCO3 Precipitation, Crystal Growth & Design, 12 (2012) 4403-4410.
[45] A. Brotchie, F. Grieser, M. Ashokkumar, Effect of Power and Frequency on Bubble-Size Distributions in Acoustic Cavitation, Physical Review Letters, 102 (2009) 084302.
[46] B.M. Borkent, M. Arora, C.-D. Ohl, N. De Jong, M. Versluis, D. Lohse, K.A. MoRch, E. Klaseboer, B.C. Khoo, The acceleration of solid particles subjected to cavitation nucleation, Journal of Fluid Mechanics, 610 (2008) 157-182.

Figure Captions

Figure 1 Reactor setup.

Figure 2 Evolution of the median particle diameter (D_{50}) for the applied frequencies in time (P_{cal} = 49 W/L). The silent and sonicated experiments were each repeated 3 and 2 times respectively.

Figure 3 Particle size distribution after 120 min for the applied frequencies (P_{cal} = 49 W/L).

Figure 4 SEM images of the samples after 120 min (P_{cal} = 49 W/L) with (a) silent, (b) 94 kHz, (c) 577 kHz and (d) 1135 kHz. With ρ_{tap} the measured tap density.

Figure 5 Improvement in tap densities for the applied frequencies and intensities. Calculated as $\frac{\rho_{son}-\rho_{sil}}{\rho_{sil}}$ with ρ_{son} the tap density under sonication (g/cm³) and ρ_{sil} the tap density under silent conditions (g/cm³).

Figure 6 Calorimetric power at different stirring speeds.

Figure 7 PSD at different ultrasonic intensities at a ultrasonic frequencies of 94 and 1135 kHz.

Figure 8 SEM images of the samples after 120 min (94 kHz) with (a) silent, (b) 4 W/L, (c) 25 W/L and (d) 49 W/L. With ρ_{tap} the measured tap density.

Figure 9 SEM images of the samples after 120 min (577 kHz) with (a) continuous and (b) pulsated irradiation.

Figure 10 PSD before and after shaping (P_{cal} = 49 W/L, f = 94 kHz).

Figure 11 SEM images during the shaping experiment (94 kHz, 49 W/L) with samples taken after (a) 1 min, (b) 5 min, (c) 10 min and (d) 15 min.

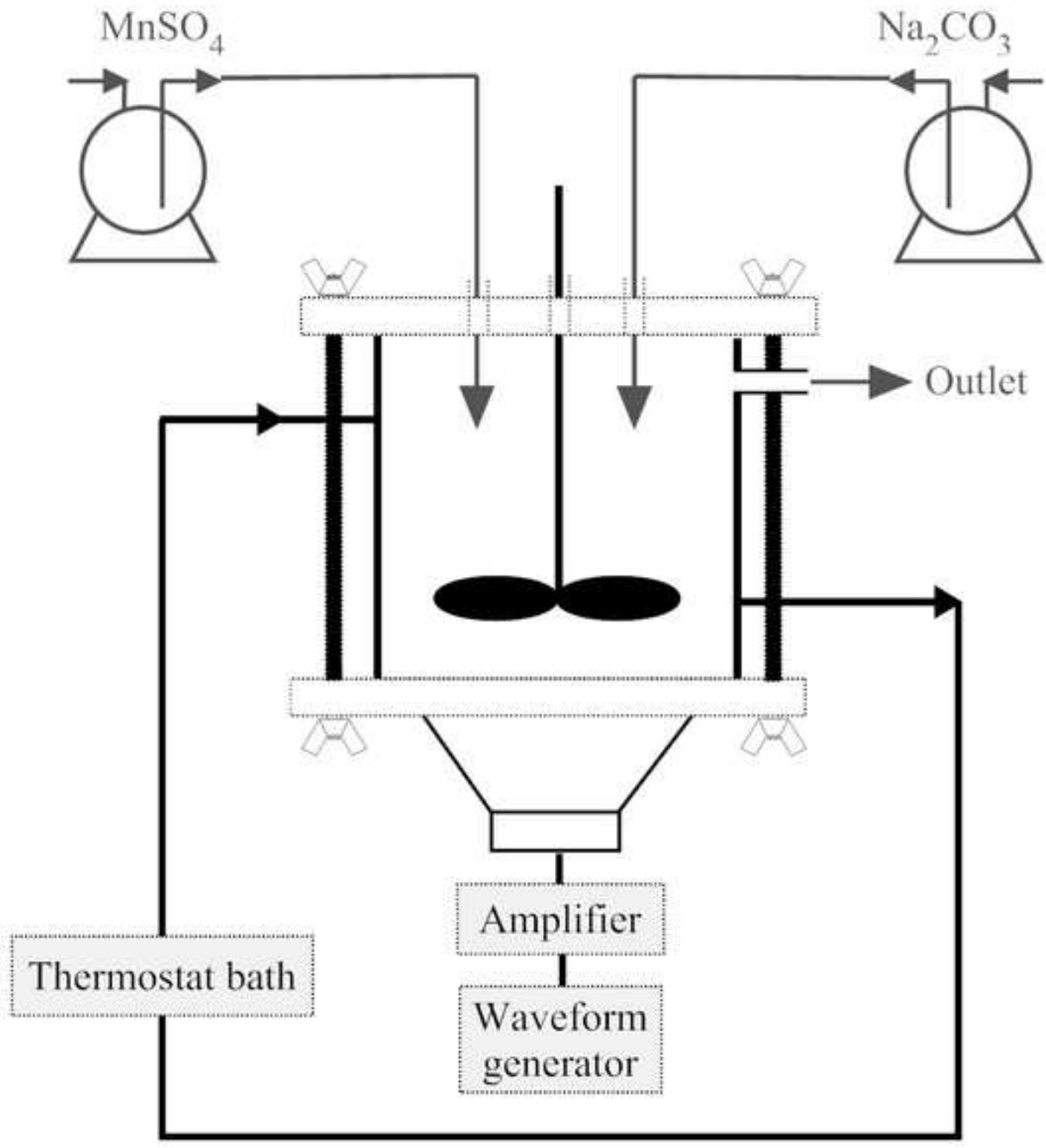
MnSO4
Na2CO3
Outlet
Amplifier
Thermostat bath
Waveform generator

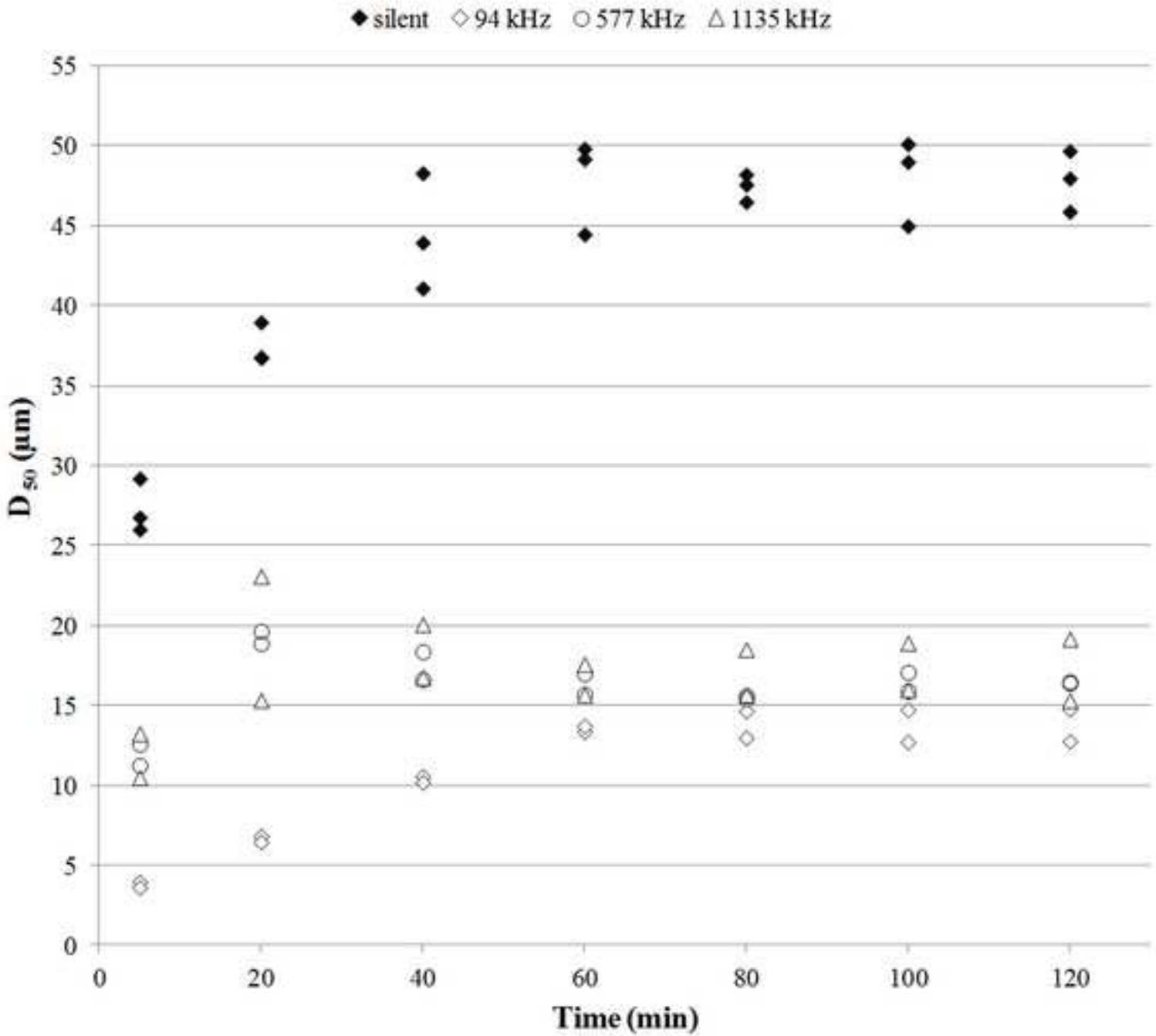

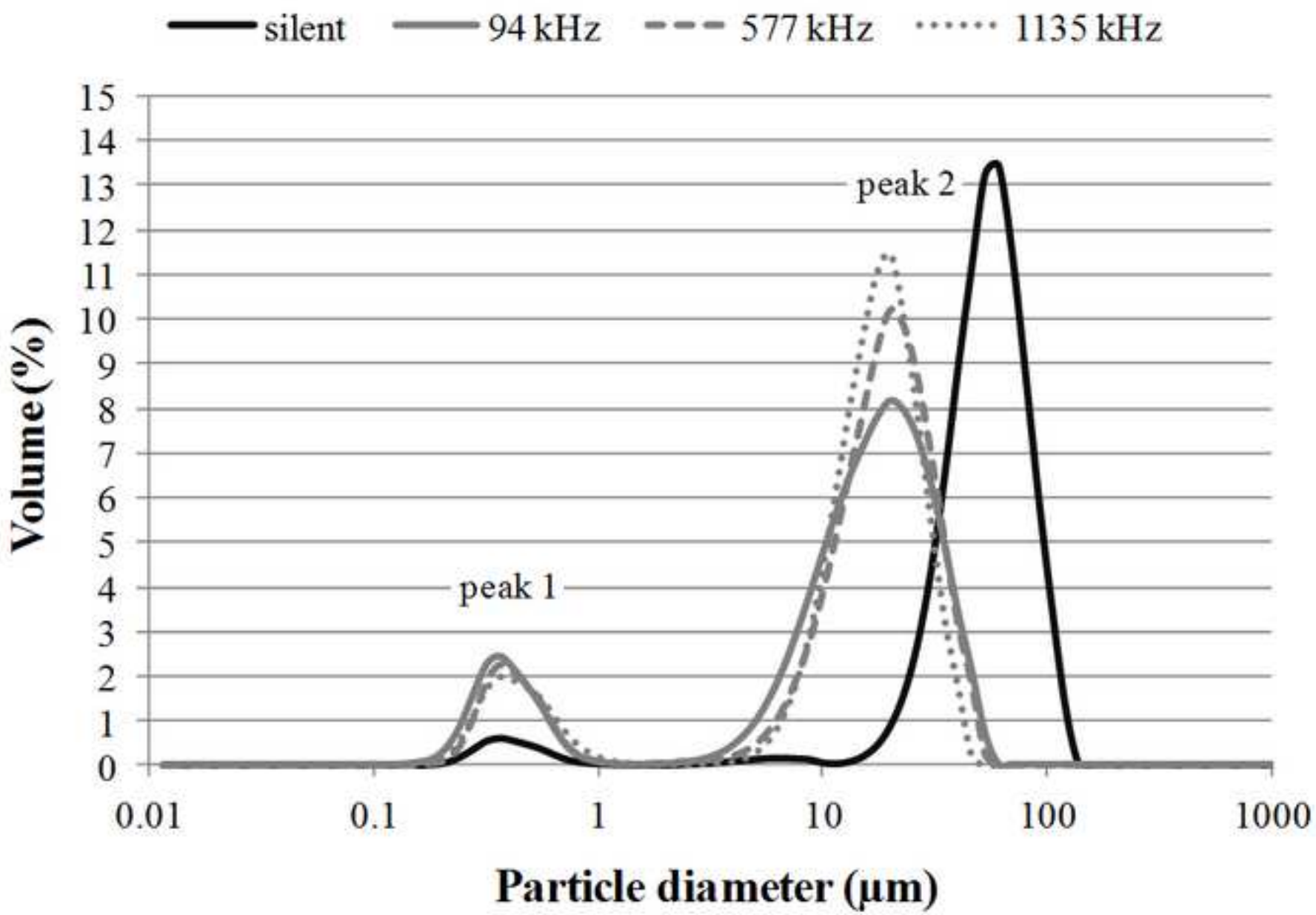

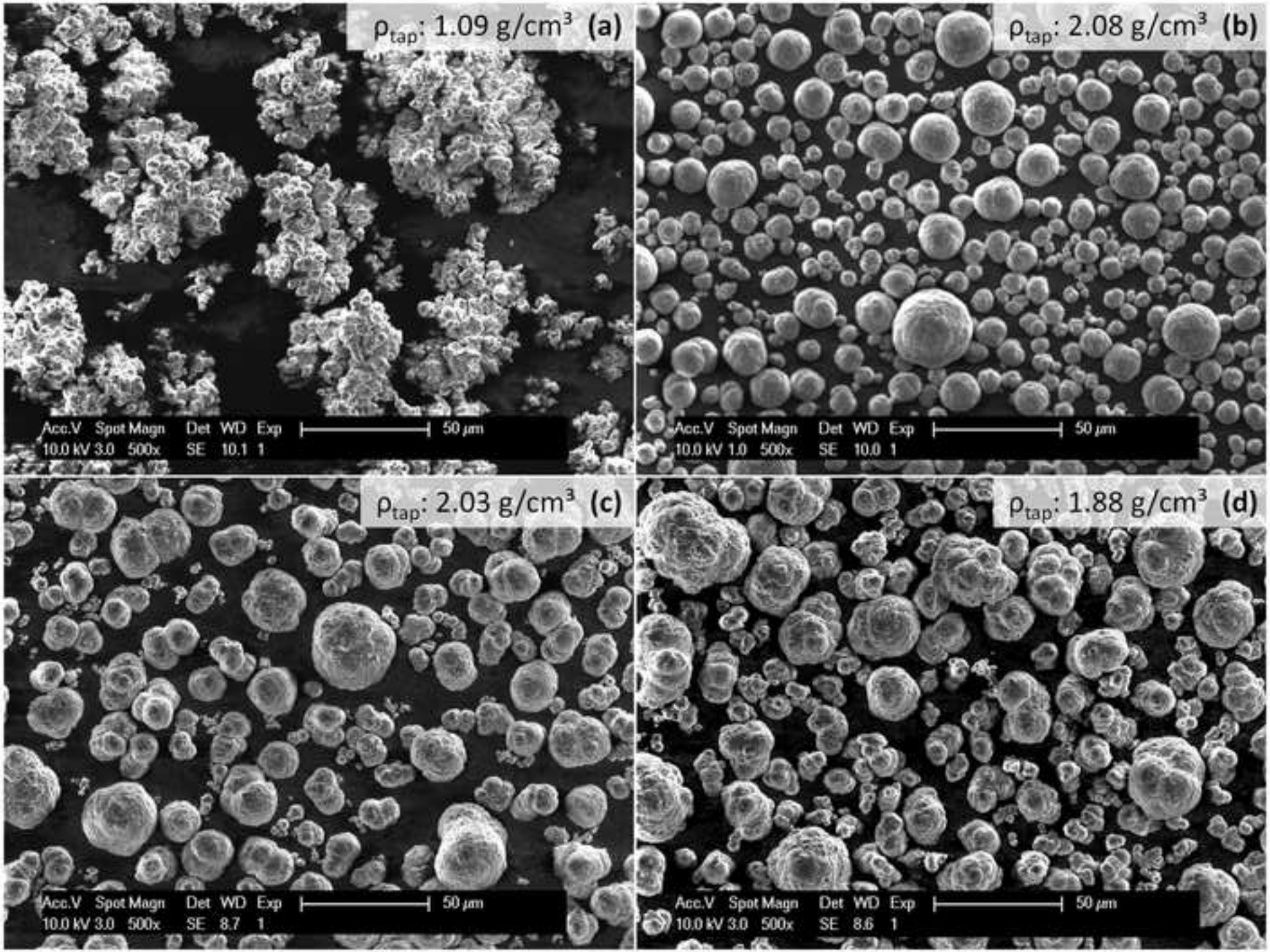

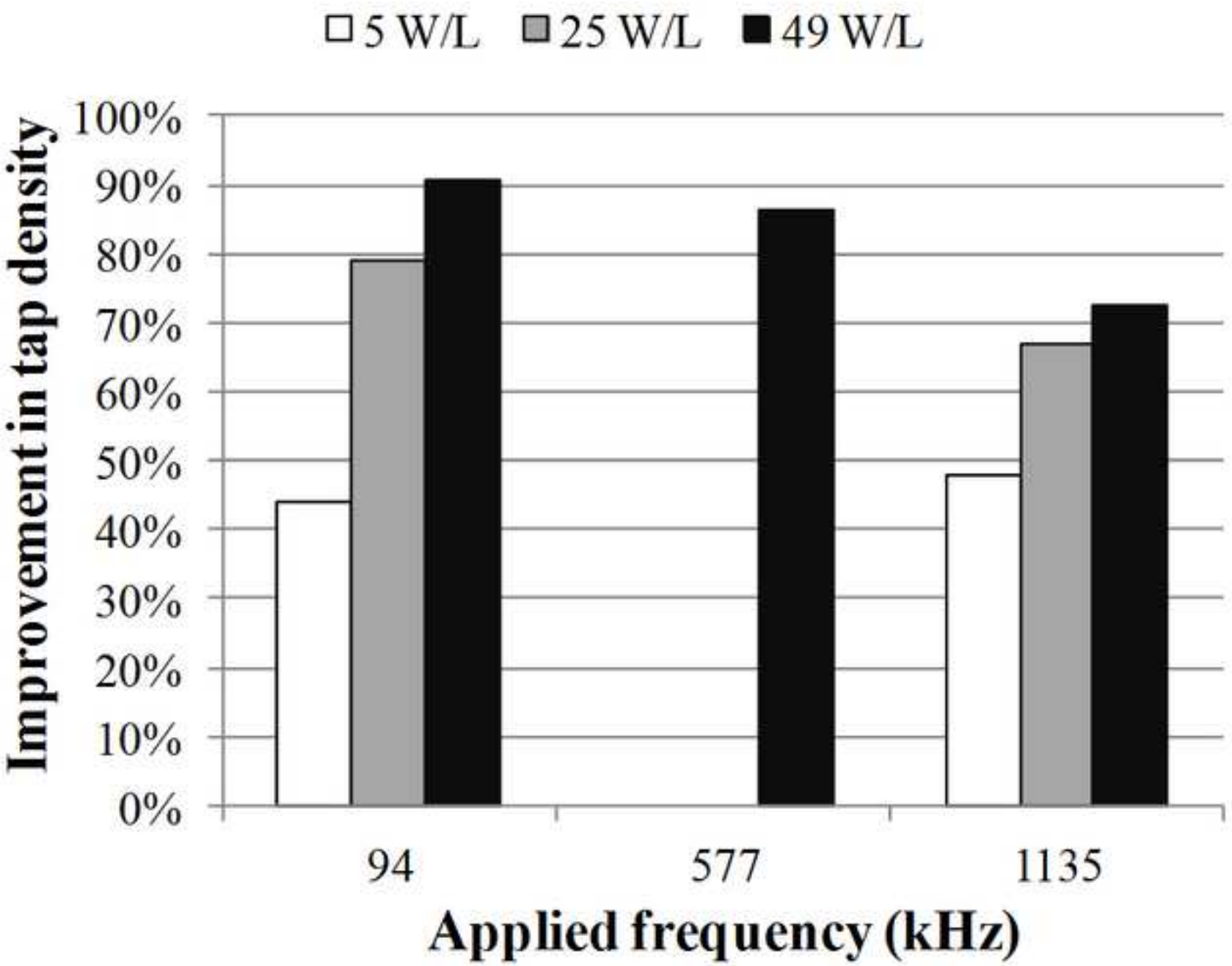

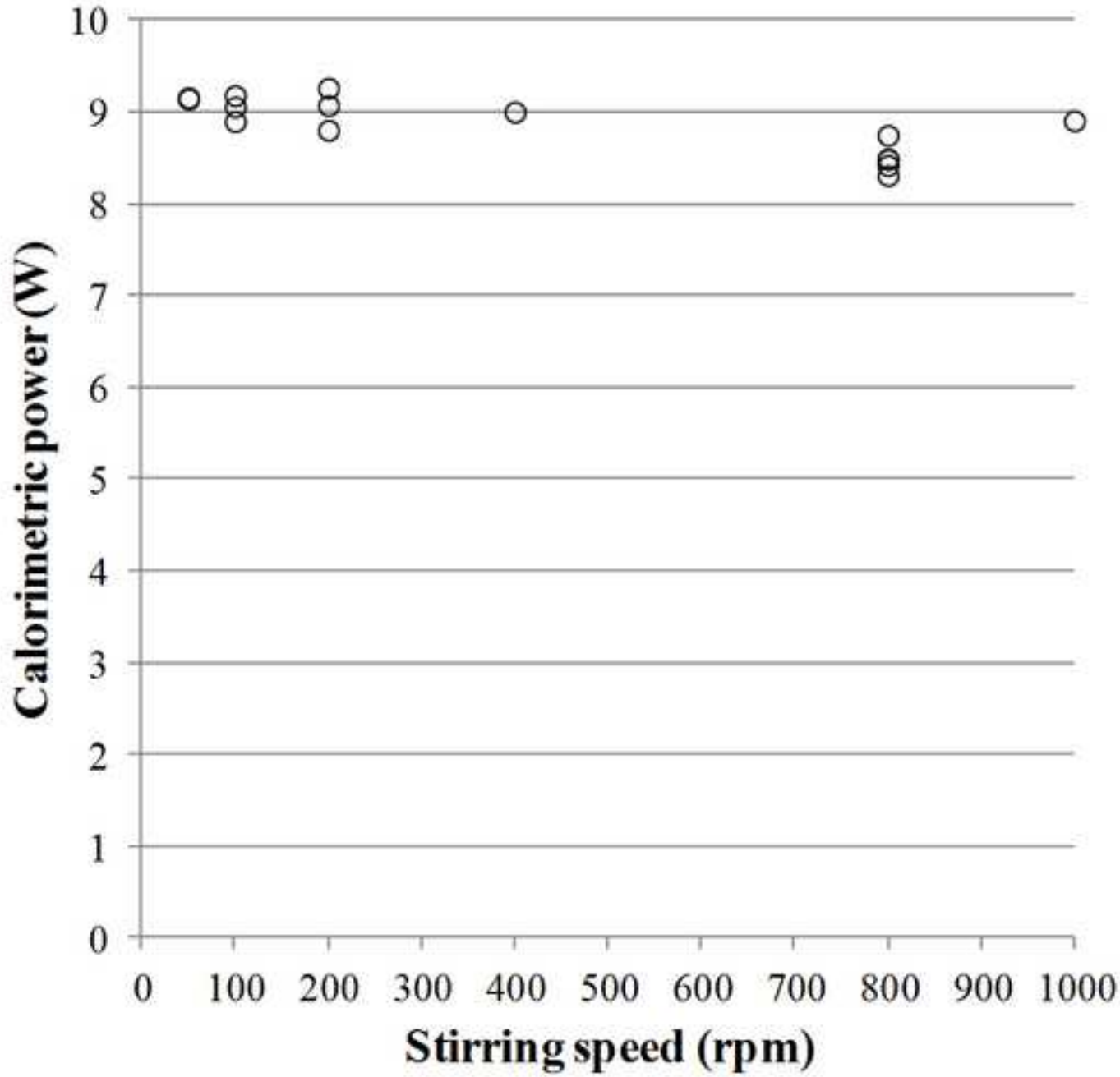

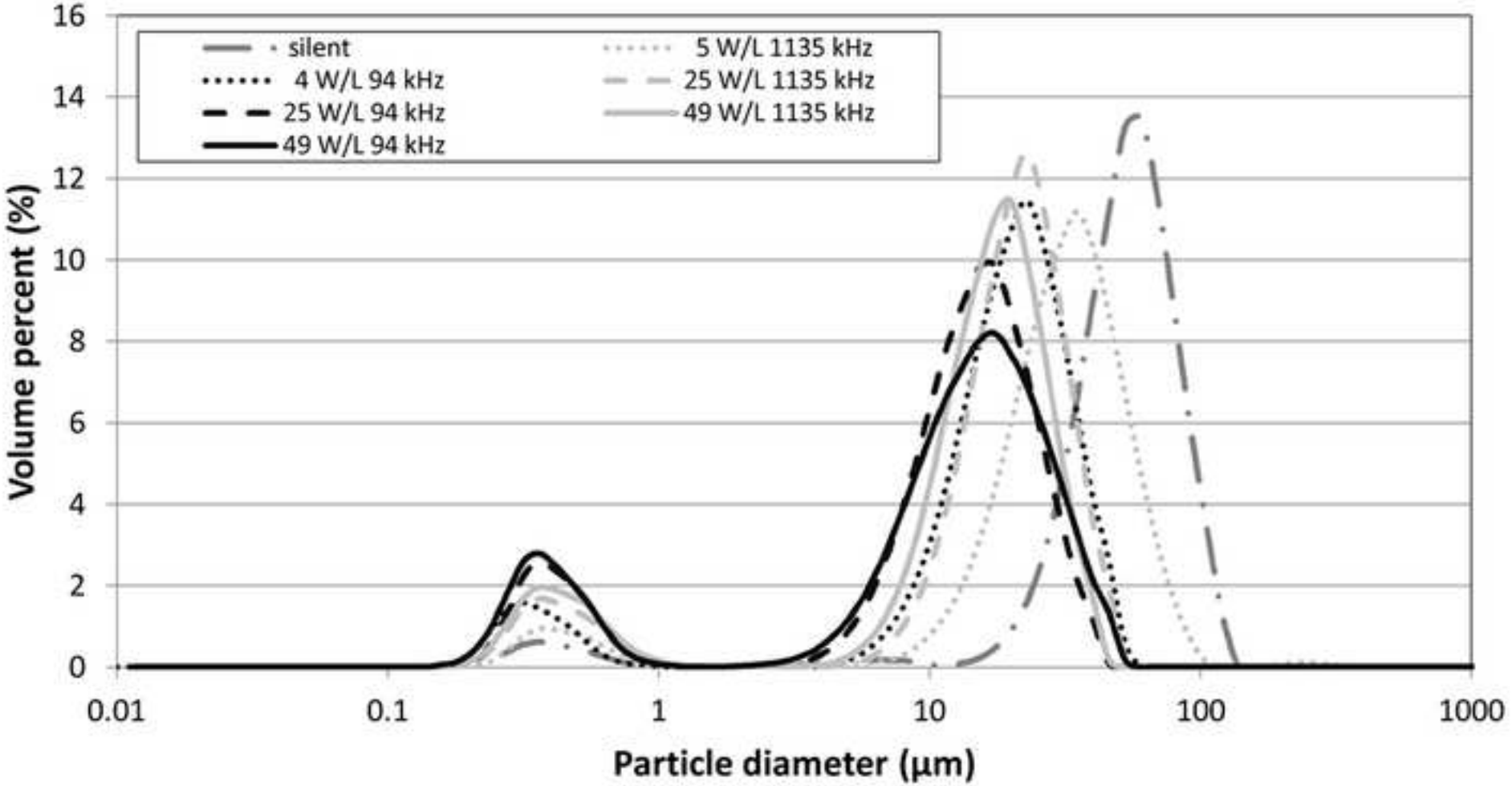

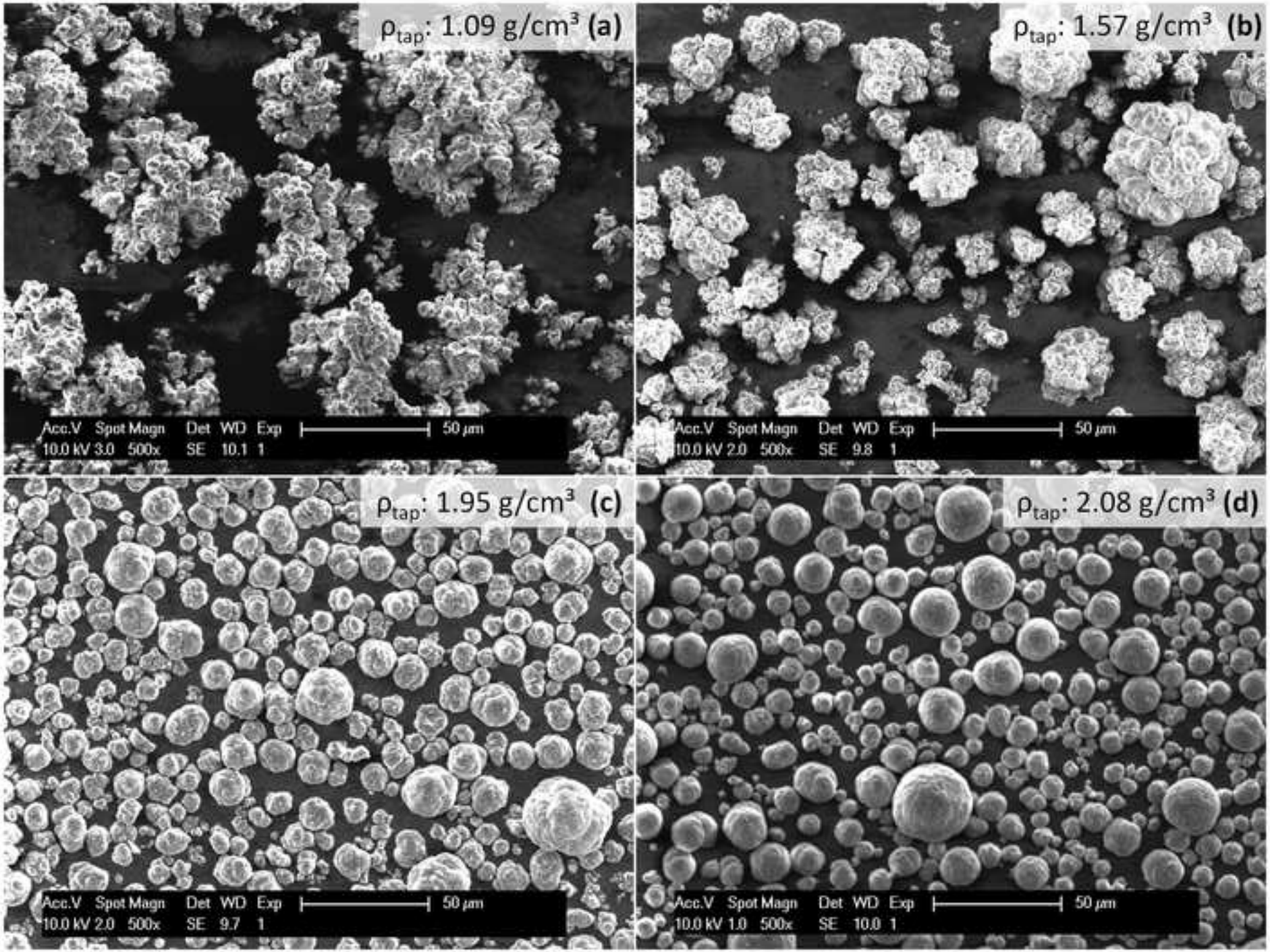

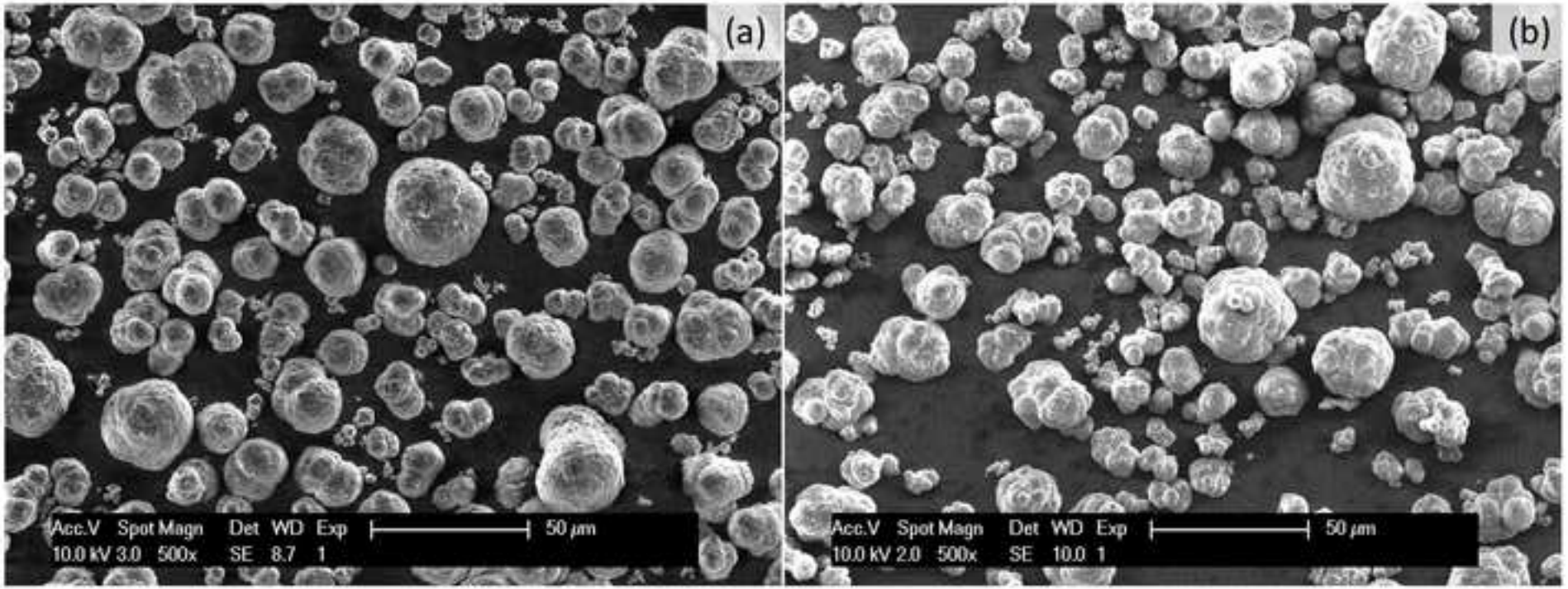

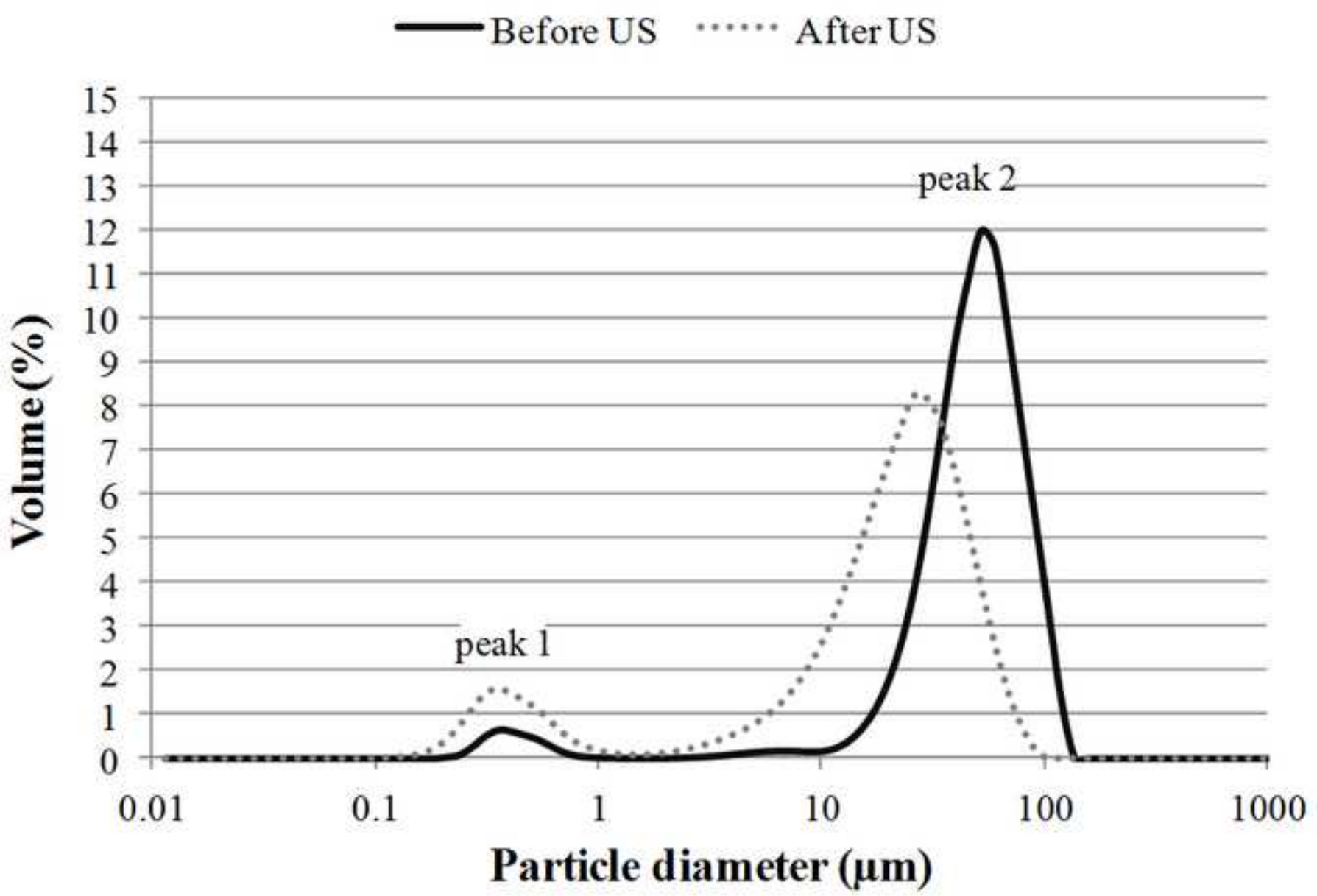
Before US
After US
Volume (%)
15
14
13
12
11
10
9
8
7
6
5
4
3
2
1
0
peak 1
peak 2
0.01
0.1
1
10
100
1000
Particle diameter (µm)

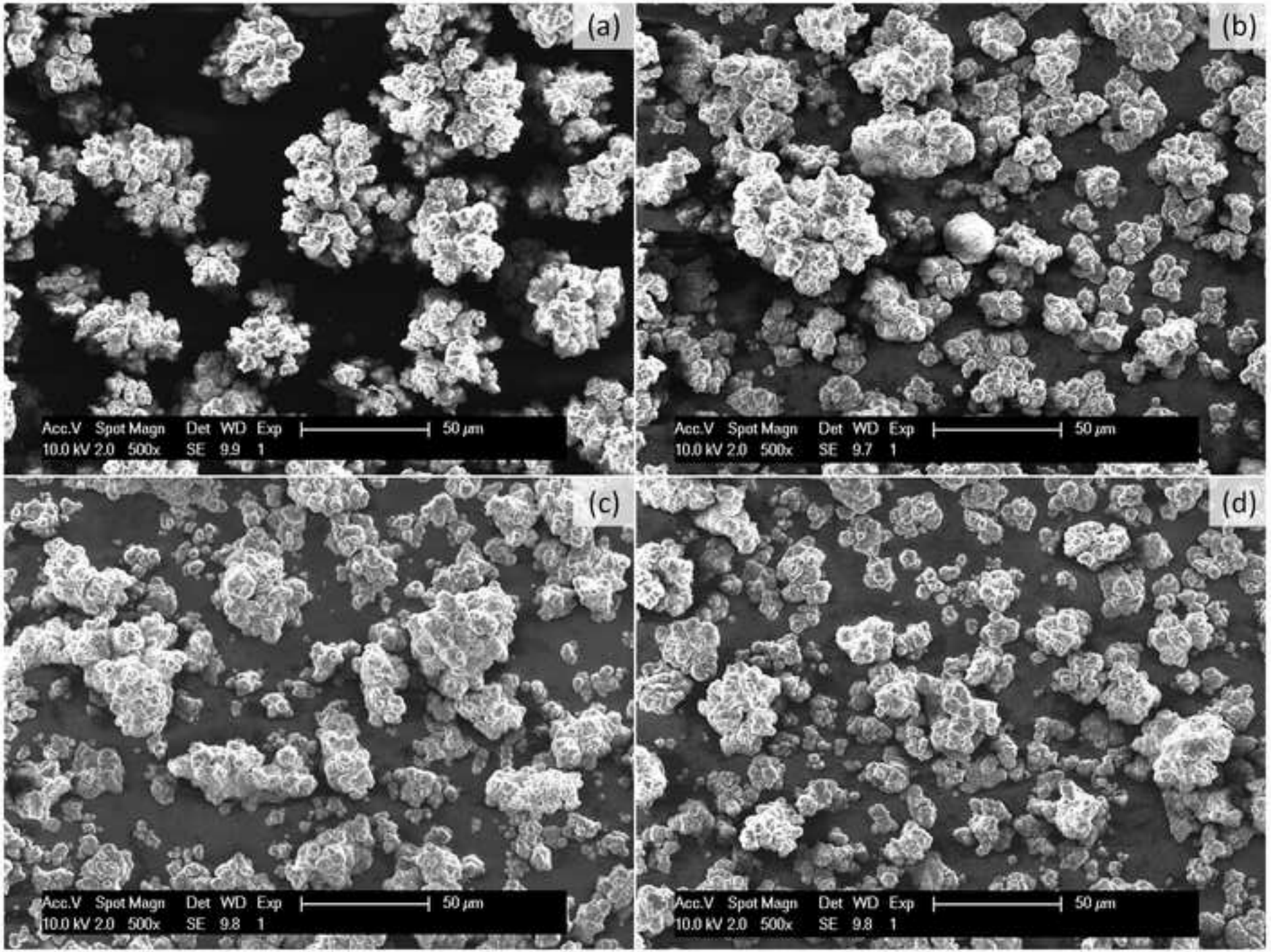

Highlights

- Particle shape influenced by both ultrasonic frequency and intensity;
- Low frequencies and elevated ultrasonic intensities preferred for the production of spherical particles with high tap densities;
- Particle size threshold exists below which particles cannot be further reduced.